A semiconductor laser system for the production of antihydrogen

2012 New J. Phys. 14 055009

(http://iopscience.iop.org/1367-2630/14/5/055009)

New Journal of Physics
The open-access journal for physics

A semiconductor laser system for the production of antihydrogen

A Müllers[1,5], S Böttner[1,6], D Kolbe[1], T Diehl[1], A Koglbauer[1], M Sattler[1], M Stappel[1], R Steinborn[1], J Walz[1], G Gabrielse[2], R Kalra[2], W S Kolthammer[2], R P McConnell[2], P Richerme[2], D W Fitzakerley[3], M C George[3], E A Hessels[3], C H Storry[3], M Weel[3], D Grzonka[4] and W Oelert[4] (ATRAP Collaboration)

[1] Institut für Physik and Helmholtz Institut Mainz, Johannes Gutenberg-Universität, 55099 Mainz, Germany
[2] Department of Physics, Harvard University, Cambridge, MA 02138, USA
[3] Department of Physics and Astronomy, York University, Toronto, ON M3J 1P3, Canada
[4] Forschungszentrum Jülich GmbH, 52425 Jülich, Germany
E-mail: mandreas@uni-mainz.de

New Journal of Physics **14** (2012) 055009 (10pp)
Received 6 January 2012
Published 9 May 2012
Online at http://www.njp.org/
doi:10.1088/1367-2630/14/5/055009

Abstract. Laser-controlled charge exchange is a promising method for producing cold antihydrogen. Caesium atoms in Rydberg states collide with positrons and create positronium. These positronium atoms then interact with antiprotons, forming antihydrogen. Laser excitation of the caesium atoms is essential to increase the cross section of the charge-exchange collisions. This method was demonstrated in 2004 by the ATRAP collaboration by using an available copper vapour laser. For a second generation of charge-exchange experiments we have designed a new semiconductor laser system that features several improvements compared to the copper vapour laser. We describe this new laser system and show the results from the excitation of caesium atoms to Rydberg states within the strong magnetic fields in the ATRAP apparatus.

[5] Author to whom any correspondence should be addressed.
[6] Present address: Leibniz Institute for Solid State and Materials Research, 01069 Dresden, Germany.

Contents

1. Introduction

Spectroscopy of antihydrogen confined in a magnetic gradient trap (Ioffe–Pritchard trap) may provide a precise test of CPT symmetry, the combined operation of charge conjugation C, parity P and time reversal T [1]. So far, antihydrogen has almost exclusively been produced by three-body recombination of an antiproton and two positrons [2, 3]. However, this method suffers from an inherent drawback: although antiprotons and positrons can be stored and cooled in the same nested Penning trap, they are then separated by a potential barrier. Overcoming this barrier requires energy to be added and therefore heats the particles. Antihydrogen atoms created this way can have temperatures much higher than the typical trap depth of neutral atom traps of 0.5 K.

Laser-controlled production of antihydrogen via double charge exchange provides an elegant solution to this problem [4]. Excited caesium atoms collide with positrons, forming positronium in Rydberg states. These positronium atoms are no longer confined by the electric potentials of the Penning trap and some will drift into the neighbouring cloud of antiprotons where, in a second charge-exchange collision, they form antihydrogen. The cross section of the charge-exchange collisions is proportional to the fourth power of the principal quantum number $n, \sigma \propto n^4$ [4]. Therefore laser excitation of the caesium atoms is crucial to increase the efficiency of the process.

This method was first demonstrated by the ATRAP collaboration in 2004 [5] at CERN's Antiproton Decelerator. Caesium and a two-stage excitation scheme were used because lasers were available. Other Rydberg atoms may be suitable as well. The first excitation step from the ground state of caesium $6S_{1/2}$ to $6P_{3/2}$ requires laser light with a wavelength of 852 nm. This was provided by a diode laser. The transition energy from this intermediate level to the closely spaced Rydberg states corresponds to a wavelength of 511 nm. For this step, a commercial copper vapour laser was used. Due to its pulsed operation (20 ns duration every 50 μs), it saturated the transition for a brief time, while no excitation happened between pulses. Laser excitation has to take place within the apparatus, close to the positrons. To limit the heat load on the cryogenic trap the pulse energy had to be limited to 0.025 mJ. The laser light crosses a collimated beam of caesium atoms at right angle (see figure 3). The Doppler width for atoms that reach the inside of the electrode stack is approximately 12 MHz. Since the copper vapour

laser had a spectral width of 6 GHz, only a fraction of the available laser power would actually excite caesium atoms.

Furthermore, the laser was not tunable, so only a single Rydberg state ($n = 37$) was accessible. Higher n-states have a much larger cross section for charge-exchange collisions and longer lifetimes, which increase the number of positronium and antihydrogen produced. On the other hand, the excitation efficiency decreases and the Rydberg atoms are Stark ionized by weaker electric fields. Due to their space charge, this ionization limits the number of positrons that can be used per experiment. Given these concerns, the ability to choose an optimum Rydberg state with a tunable laser is a great advantage.

For a second improved generation of charge-exchange experiments, we wanted to replace the copper vapour laser with a tunable narrow-linewidth continuous-wave laser system. For operation at an accelerator facility, a compact, reliable low-maintenance system is especially important. Therefore we chose a frequency-doubled semiconductor master-oscillator power-amplifier (MOPA) laser system. Designing a custom system promised higher output powers than the 50 mW available from commercial lasers at the time.

Section 2 of this paper describes the lasers used for two-stage excitation of caesium and the components for producing a beam of caesium atoms within the ATRAP apparatus. In section 3, we present the results from laser excitation of caesium to Rydberg states in the strong magnetic fields required for our Penning and Ioffe traps.

2. The laser system

2.1. The 852 nm laser

The setup for the excitation of the first transition $6S_{1/2} \rightarrow 6P_{3/2}$ (Cs D_2 line) is shown in figure 1. The laser source is an external cavity diode laser (ECDL) with a feedback grating in the Littrow configuration similar to [6]. The linewidth of this type of laser is approximately 1 MHz. We are using a laser diode from the Frankfurt Laser Company (FIDL-200S-850X) with a maximum output power of 200 mW. A few milliwatts are sufficient to saturate this transition, so the diode can be operated at about half its maximum current of 300 mA. The wavelength of the laser is controlled by the angle of the feedback grating. Coarse tuning can be done manually with a fine-threaded screw and a piezo actuator is used for fine-tuning. The voltage applied to the piezo is also fed into a modulation input of the laser diode's current driver (feed-forward). With this setup, a mode-jump-free tunability of up to 50 GHz is achieved. The piezo is also used to lock the laser to the desired frequency utilizing a wavemeter (see section 2.3). A Faraday isolator with 60 dB attenuation (Linos DLI-1) protects the diode from back reflections. Two beam samplers split off small parts of the main beam. The first sampled beam is divided between a fibre coupler that sends light into the wavemeter, while the other half is used to record the laser power with a photodiode. The light from the second beam sampler is sent into a setup for Doppler-free saturation spectroscopy in a magnetically shielded caesium vapour cell. This is used as the frequency reference for the wavemeter.

2.2. The 511 nm laser

For the second transition from the $6P_{3/2}$ level to Rydberg states, we wanted to replace the pulsed copper vapour laser with a tunable continuous-wave laser system. The saturation intensities for

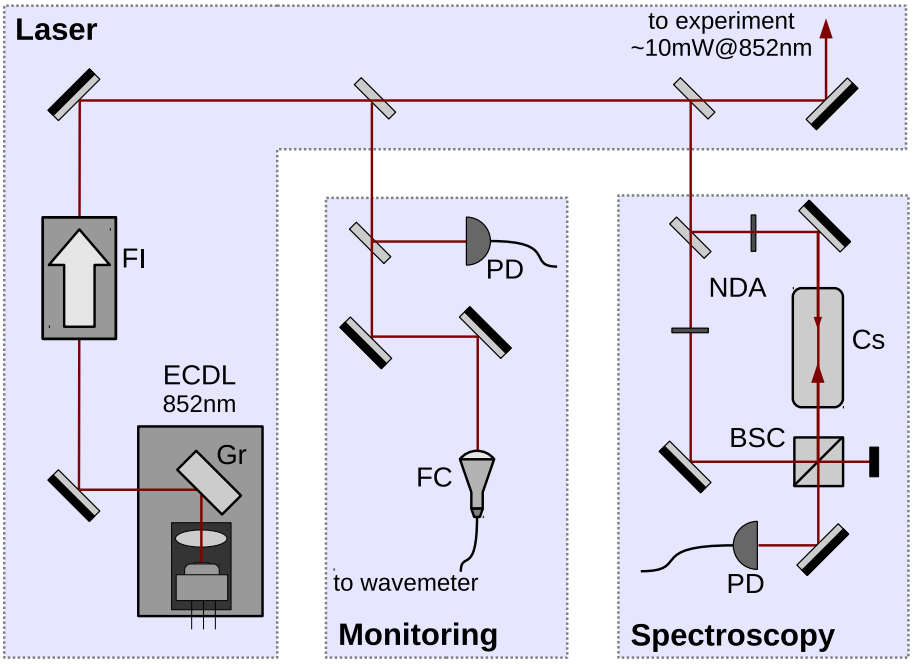

Figure 1. The first laser system for excitation of caesium from the ground state to the $6P_{3/2}$ state. ECDL, external cavity diode laser; Gr, grating; FI, Faraday isolator; PD, photodiode; FC, fibre coupler; NDA, neutral-density attenuator; Cs, caesium vapour cell; BSC, non-polarizing beam splitter cube.

these transitions are much higher than those for the first one, so more power is required for an efficient excitation. We designed an MOPA system based on semiconductor lasers operating at a wavelength of 1022 nm and a frequency-doubling resonator to convert this light into the required wavelength of 511 nm. The system is shown in figure 2. The first component is again an ECDL. The laser diode used is an Eagleyard EYP-RWE-1060 with a maximum output power of 100 mW. Its front facet is antireflection coated, which increases the stability of the laser modes and provides better tunability. A Faraday isolator with 60 dB attenuation (Linos FI-1060-TI) protects the diode against back reflections. Part of the beam is split off to monitor the wavelength. About 20 mW of laser power is used to seed a tapered amplifier (m2k TA-1030-1000) with an output power of 1 W. Incoupling and outcoupling of the beam are done with two $f = 3.7$ mm lenses mounted on three-axis movable stages (Newport M-DS-25-XYZ). A cylindrical lens corrects the astigmatism of the amplifier's output beam and an additional telescope reduces the beam diameter to increase transmission through a second Faraday isolator (the same type as above). The light deflected from this isolator's input polarization filter is recorded with a photodiode as a power reference.

Two lenses on movable stages match the beam's focus size and divergence to a compact resonator for frequency doubling. It consists of two curved 1/2 inch mirrors ($r = 38$ mm) for incoupling and outcoupling, a nonlinear crystal and a prism. The prism replaces two of the mirrors in the common bow-tie resonator design [7]. This triangular geometry allows a short round-trip path length of only 16 cm. Short path lengths reduce beam pointing from distortions of the optical components and thus increase the resonator's stability. The prism is mounted on a piezo actuator, which is used to stabilize the cavity length to be resonant with the wavelength

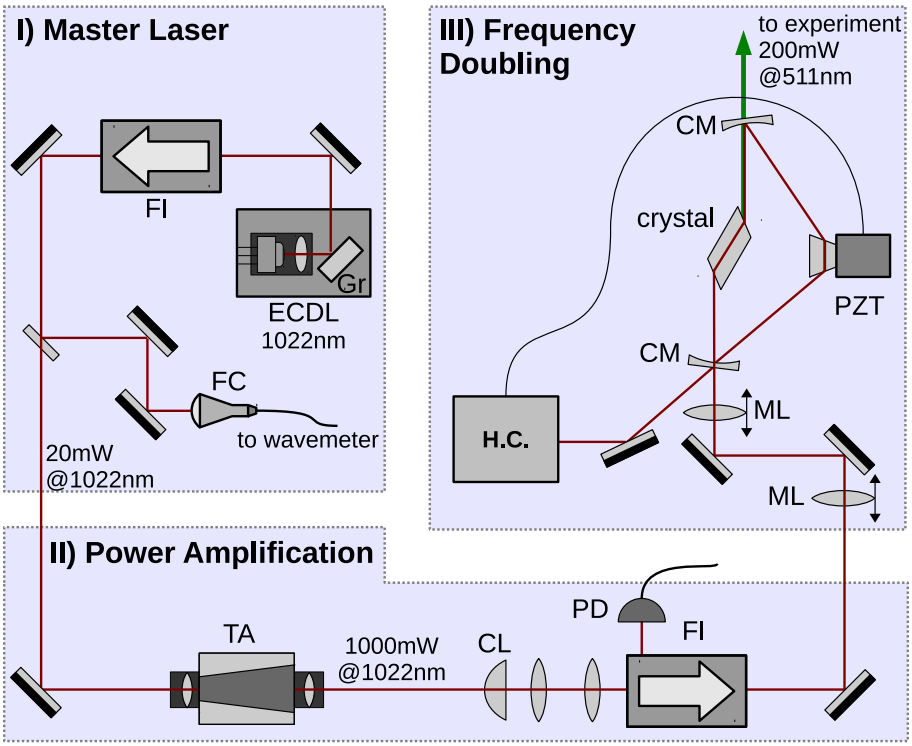

Figure 2. The second laser system for the excitation from the $6P_{3/2}$ intermediate level to Rydberg states. ECDL, external cavity diode laser; Gr, grating; FI, Faraday isolator; PD, photodiode; FC, fibre coupler; TA, tapered amplifier; CL, cylindrical lens; ML, movable lens; CM, cavity mirror; PD, photodiode; PZT, piezo actuator; H.C., components for Hänsch–Couilleaud lock.

of the fundamental beam. We use a Hänsch–Couilleaud-type lock [8]. About 60% of the fundamental light is coupled into the cavity. This value is limited by the tapered amplifier's beam quality. The nonlinear crystal is cut at Brewster's angle for type I critical phase matching. It is heated to $T = 313$ K to prevent the deposition of atmospheric water vapour on its surfaces. For the nonlinear medium we compared lithium triborate (LBO) and bismuth boron oxide (BiBo). BiBo has a four times higher nonlinear coefficient than LBO but also suffers from a larger walk-off angle. With an LBO crystal (10 mm length) we generated about 50 mW of output power with a wavelength of 511 nm. Installing a BiBo crystal (8 mm length) increased the available output power to 200 mW. This corresponds to an optical conversion efficiency of 39%. We achieved a mode-jump-free tunability of more than 20 GHz. The overall tuning range is limited by the tapered amplifier's gain region from 1000 to 1040 nm. This allows us to access all caesium states from $n \simeq 20$ (520 nm) up to the ionization limit (508 nm).

2.3. Frequency stabilization

Laser excitation takes place within strong magnetic fields of 1 T or more, which influence the atomic states of the caesium atoms (see section 3). Therefore, we cannot lock the lasers to a caesium vapour cell since the same large magnetic field is not available on a laser table. Instead, we are using a wavemeter (High Finesse WS7). We have observed a temperature dependence of

the measured frequency of about 10 MHz K^{-1}. To prevent large drifts over time, the wavemeter is placed in a temperature-stabilized housing, which reduces the temperature fluctuations to below 0.1 K.

Software running on a standard computer reads out the wavemeter and calculates error signals for both lasers using a proportional-integral-derivative controller loop. These signals are converted into voltages and supplied to the piezos controlling the grating angles for the laser diodes via a multi-purpose measurement card (Meilhaus ME4660, 2 analogue outputs, 16 analogue inputs). An optical switcher connected to the wavemeter allows both lasers to be locked simultaneously. Stable operation is achieved for hours. The same software and measurement card are also used for data acquisition and monitoring the laser powers and frequencies.

2.4. Experimental setup

The two laser beams are superimposed with a dichroic mirror and coupled into the same multimode fibre (Thorlabs M31L10). Due to the fibre's large core diameter of 62.5 μm, an incoupling efficiency of more than 70% is achieved for both lasers simultaneously. The fibre guides the laser light to the excitation region within our cryogenic apparatus. Even when running at full power for up to an hour, no heating of the trap electrodes from the lasers is observed.

Figure 3 shows the main components used for caesium excitation and charge-exchange experiments. The rest of the ATRAP apparatus is described in more detail in [9]. A beam of caesium atoms is emitted from a commercial alkali-metal dispenser (ALVATEC AS-3-Cs-150-V). The source is placed inside an enclosure for radiation shielding. The laser light is collimated to a beam of 1.5 mm diameter. It crosses the beam of caesium atoms at right angle. The fluorescence from the relaxation of the $6P_{3/2}$ state is recorded with an indium-gallium-arsenide (InGaAs) photodiode. This signal is used to tune the 852 nm laser to resonance. To detect excitation to Rydberg states, a field ionization setup is used. An electric field strong enough to ionize high-n states is generated by a voltage on one of two conducting plates and the resulting current onto the other plate is measured. The collimation baffles are designed to ensure that all caesium atoms which enter the electrode stack through a 0.8 mm hole will leave again through a 2.5 mm hole on the opposite side. This prevents the build-up of caesium inside the electrode stack. For charge-exchange experiments, positrons are stored on the electrode crossed by the caesium beam and antiprotons on one of the neighbouring electrodes. The apparatus is placed within a large superconducting 1 T solenoid for radial confinement of the charged antiprotons and positrons. A superconducting quadrupole Ioffe trap for the storage of antihydrogen creates additional magnetic fields including an inhomogeneous component from the quadrupole coils.

3. Results

For the first transition from the ground state $6S_{1/2} \rightarrow 6P_{3/2}$, the change of the caesium energy levels from magnetic fields can be calculated using the Breit–Rabi formula. Due to the nuclear angular momentum of caesium of $I_{Cs} = 7/2$, each of the six hyperfine transition lines splits up into eight magnetic lines ($m_I = -7/2, -5/2, \ldots, 7/2$), separated by about 1 GHz. Figure 4 shows the fluorescence recorded with the InGaAs photodiode for the group of closed-cycle transitions $|J = 1/2, m_J = 1/2\rangle \rightarrow |J' = 3/2, m'_J = 3/2\rangle$ in the 1 T field of our Penning trap (a) and a superimposed Ioffe field of 3.6 T (b). The inhomogeneity of the quadrupole field causes a slight broadening of the lines in the second case.

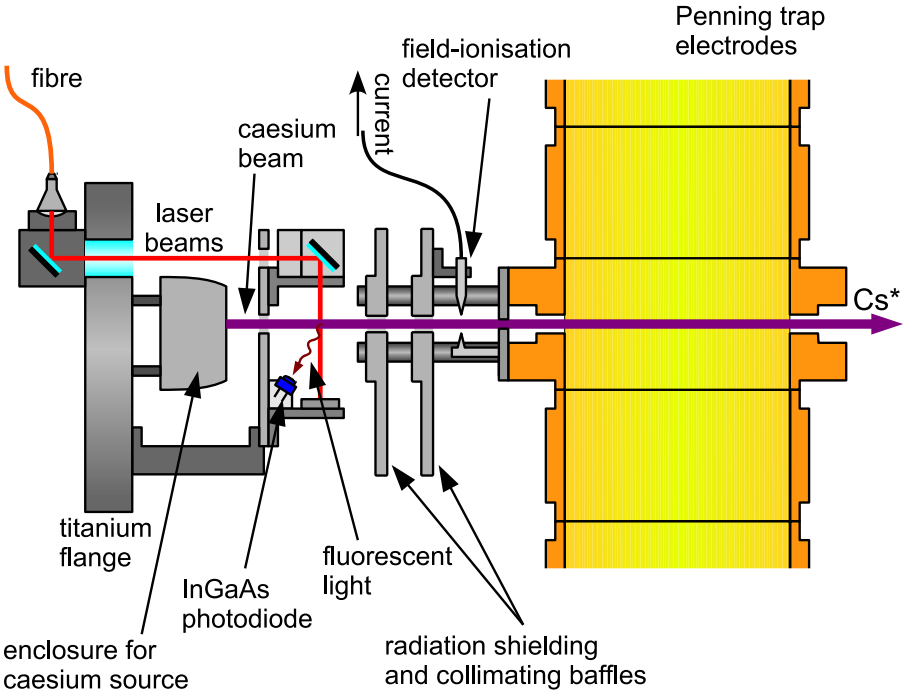

Figure 3. Schematic drawing of the components for producing a beam of Rydberg caesium atoms in the ATRAP apparatus. Caesium atoms from an alkali metal dispenser are collimated to a thin beam and laser excited before entering the Penning trap through a small hole in one of the electrodes. The 852 nm laser is tuned to resonance by maximizing the fluorescence light recorded with an InGaAs photodiode. The excitation to Rydberg states is detected and maximized with a field ionization detector.

For the weakly bound Rydberg levels the magnetic field couples states with $\Delta l = 0, \pm 2$ regardless of n. So far no analytical solution has been found for this problem. However, we could estimate the energy levels by diagonalizing a hydrogen-like Hamiltonian operator containing all relevant zero-field states from $n = 10$ to $n = 60$. The wave functions included quantum defects from [10]. This method worked well for states around $n = 42$ in the 1 T field. For higher-n states or stronger magnetic fields more zero-field states have to be included in the Hamiltonian, which causes much longer computational time and makes the method impractical. In these cases we used a semi-classical approach similar to [11]. Figure 5 shows the deviation of our calculated results from the measured frequencies $\Delta\nu = \nu_{\mathrm{calc}} - \nu_{\mathrm{meas}}$ for a number of caesium Rydberg states between $n = 37$ and $n = 50$ in a 1 T field. The energy levels range from about 2.7 THz ($n = 37$) to 1.2 THz ($n = 50$) below the ionization limit (941.54 THz). For most states both methods yield good results with an uncertainty of 5 GHz or below. For $n = 50$, diagonalization of the Hamiltonian results in an error of almost 90 GHz because not enough zero-field states were included in the calculation. It is not clear why the deviation for the $n = 46$ state is larger than that for the surrounding states. By one of these two methods, we were able to calculate the energy levels and therefore the transition frequencies within an uncertainty of a few GHz for various states in the magnetic fields of our Penning and Ioffe traps. This uncertainty is well within the tuning range of our lasers.

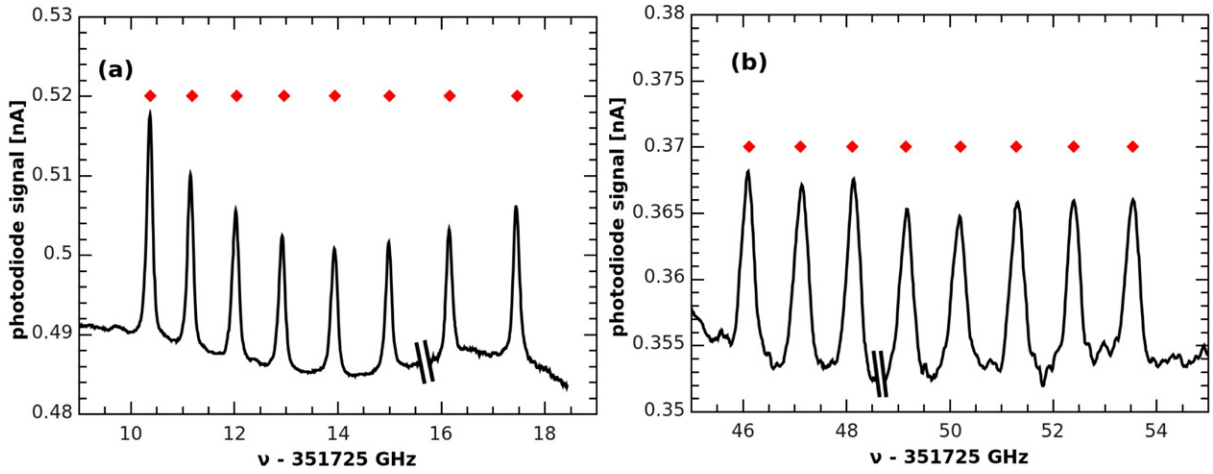

Figure 4. Fluorescence signal recorded from the group of closed cycle transitions $|J = 1/2, m_J = 1/2\rangle \rightarrow |J' = 3/2, m'_J = 3/2\rangle$ in a magnetic field of 1 T (a) and a superimposed Ioffe field of 3.6 T (b). The diamonds show the calculated transition frequencies using the Breit–Rabi formula. The double slashes indicate where the laser had to be retuned to cover the entire group. The background is caused by scattered light from the laser.

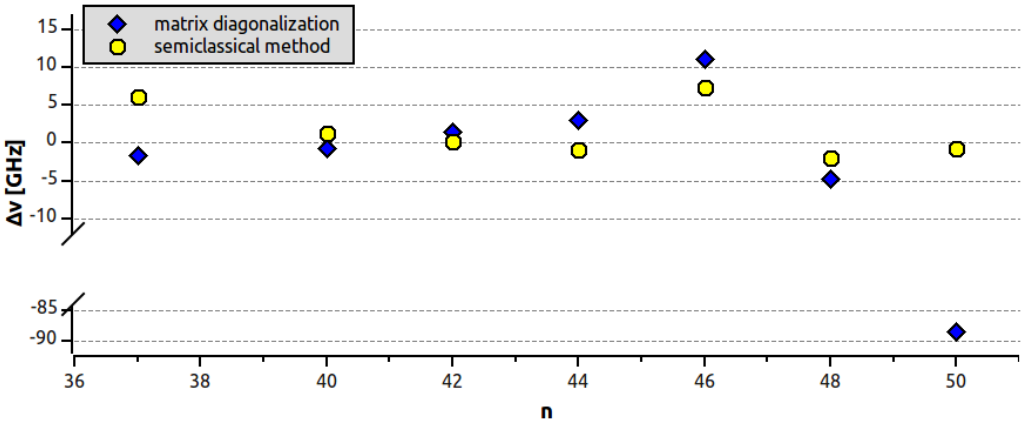

Figure 5. Deviation of the frequencies calculated by the two methods described in the text from experimental data $\Delta\nu = \nu_{\text{calc}} - \nu_{\text{meas}}$ for a number of nD Rydberg states in a 1 T field.

Figure 6 shows the current recorded from the field ionization detector when sweeping the amplitude of the electric field in the 1 T Penning trap field (a) and in the Ioffe field (b). Without a magnetic field, the excited states would correspond to 42D (a) and 38D (b), respectively. Depending on the direction of the field, we collect either negative electrons or positive caesium ions. Similar data obtained with the copper vapour laser can be found in [12], where a maximum ion current of 40 fA was measured from the $n = 38$ state in a uniform 4.9 T magnetic field. With our new laser system we achieve a value 12 times higher in our Penning trap field (figure 6(a)) and three times higher in the Ioffe field (b). However, the influence of the magnetic field should be noted. A larger field causes stronger mixing of different l states, which reduces the

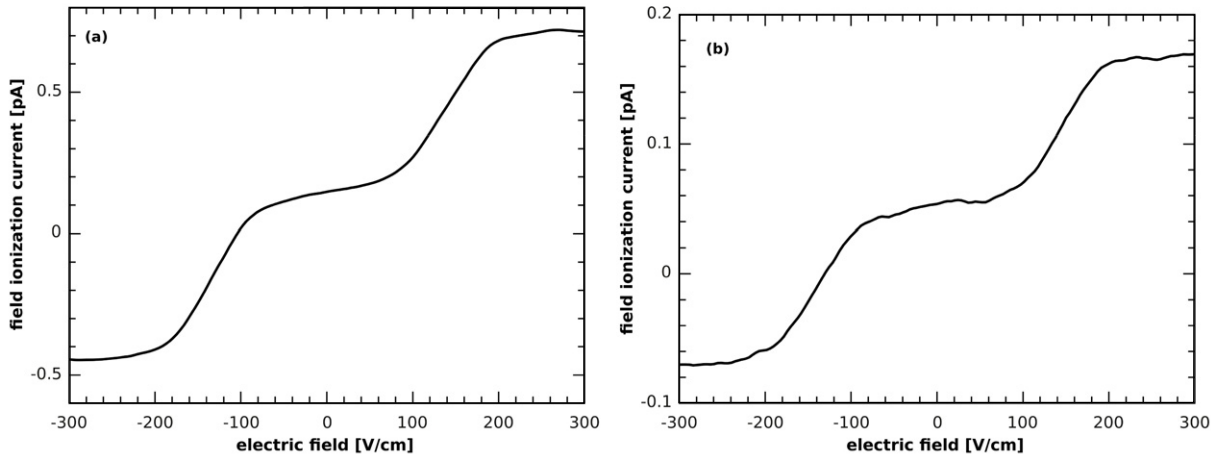

Figure 6. Field ionization current recorded when sweeping the electric field for the transitions from the $6P_{3/2}$ state to Rydberg states. (a) Excitation to the $n = 42$ state in a 1 T field and (b) excitation to the $n = 38$ state with the Ioffe trap energized to 3.2 T.

contribution of the S and D orbitals to the final magnetic field state. Therefore the excitation efficiency decreases and the factor of 12 from figure 6(a) would be somewhat reduced in a stronger field. On the other hand, the inhomogeneous quadrupole field of our Ioffe trap causes additional broadening of the transition lines, so in a homogeneous field of similar magnitude we would observe a stronger signal than in figure 6(b). Also, the observed ion current depends on the amount of ground state caesium crossing the laser beams. This is controlled by the current sent through the caesium oven. In a typical experiment we send a stream of $2 \times 10^6\,\mathrm{Cs}^*\,\mathrm{s}^{-1}$ into our trap, 2.5 times higher than in the previous experiment [5]. Due to the higher excitation efficiency, we achieve this larger stream of Rydberg atoms with much lower usage of caesium. This reduces the heat load on the cryogenic system and the deposit of caesium on the collimation baffles. Furthermore, this allows us to operate our trap for several months without the need to warm up the apparatus and break vacuum to exchange the caesium source.

The curves show a small offset at zero electric field. We seem to collect some positive caesium ions while the lighter electrons escape. We took great care not to expose any dielectric materials to the caesium beam and to ground all conducting components to prevent the build-up of electric charges that could ionize Rydberg atoms. Instead, this effect may originate from an imperfect collimation of the caesium beam or a slight misalignment of the field ionization components. If Rydberg caesium atoms hit an edge of one of the plates, they may ionize on collision. This should lead to deposition of caesium on the field ionization plate, but in very small quantities. Actually, no deposition of caesium is visible behind the first collimation baffle at all (see figure 3).

4. Conclusion

We have described a two-stage continuous-wave semiconductor laser system for the excitation of caesium atoms to Rydberg states. Both lasers feature ample tunability to find the caesium resonances in strong magnetic fields of several tesla. The frequency-doubled MOPA system

offers access to a wide range of Rydberg states. Due to its narrow linewidth of $\simeq 1$ MHz, all of its output power of 200 mW is usable for the excitation of caesium. These are major improvements compared to the previous pulsed laser system. The excitation of caesium to the $6P_{3/2}$ and to various high-n Rydberg states in magnetic fields of several tesla is demonstrated. Both lasers have shown reliable operation in the ATRAP experiment at CERN's Antiproton Decelerator.

Acknowledgments

This work was supported by a PhD scholarship from Carl Zeiss Stiftung. Funding was provided by the German Federal Ministry of Research (BMBF), Deutsche Forschungsgemeinschaft (DFG), the National Science Foundation (NSF) and Air Force Office of Scientific Research (AFOSR) of the US, the Natural Sciences and Engineering Research Council (NSERC), Canada Research Chair (CRC) and the Canada Foundation for Innovation (CFI) of Canada.

References

[1] Gabrielse G 1987 *Fundamental Symmetries* ed P Bloch, P Pavlopoulos and R Klapisch (New York: Plenum)
[2] Gabrielse G *et al* 2002 Background-free observation of cold antihydrogen with field-ionization analysis of its states *Phys. Rev. Lett.* **89** 213401
[3] Amoretti M *et al* 2002 Production and detection of cold antihydrogen atoms *Nature* **419** 456–9
[4] Hessels E A, Homan D M and Cavagnero M J 1998 Two-stage Rydberg charge exchange: an efficient method for production of antihydrogen *Phys. Rev.* A **57** 1668–71
[5] Storry C H *et al* 2004 First laser-controlled antihydrogen production *Phys. Rev. Lett.* **93** 263401
[6] Ricci L, Weidemüller M, Esslinger T, Hemmerich A, Zimmermann C, Vuletic V, König W and Hänsch T W 1995 A compact grating-stabilized diode laser system for atomic physics *Opt. Commun.* **117** 541–9
[7] Zanger E, Müller R, Liu B and Gries W 1999 Diode-pumped industrial high-power cw all-solid state laser at 266 nm *SPIE Conf. Proc.* **3862** 255–61
[8] Hänsch T W and Couillaud B 1980 Laser frequency stabilization by polarization spectroscopy of a reflecting reference cavity *Opt. Commun.* **35** 441–4
[9] Gabrielse G *et al* 2007 Antiproton confinement in a Penning–Ioffe trap for antihydrogen *Phys. Rev. Lett.* **98** 113002
[10] Weber K H and Sansonetti C J 1987 Accurate energies of nS, nP, nD, nF and nG levels of neutral cesium *Phys. Rev.* A **35** 4650–60
[11] Economou N P, Freeman R R and Liao P F 1978 Diamagnetic structure of Rb in intense magnetic fields *Phys. Rev.* A **18** 2506–9
[12] Speck A, Storry C H, Hessels E A and Gabrielse G 2004 Laser-controlled production of Rydberg positronium via charge exchange collisions *Phys. Lett.* B **597** 257–62